Inorganic Chemistry

Article

pubs.acs.org/IC

Exploration of Mid-Temperature Alkali-Metal-Ion Extraction Route Using PTFE (AEP): Transformation of α-$NaFeO_2$-Type Layered Oxides into Rutile-Type Binary Oxides

Tadashi C. Ozawa*[,†,‡] and Takayoshi Sasaki[†,‡]

[†]International Center for Materials Nanoarchitectonics (WPI-MANA), National Institute for Materials Science (NIMS), 1-1 Namiki, Tsukuba, Ibaraki 305-0044, Japan

[‡]CREST, Japan Science and Technology Agency (JST), 4-1-8 Honcho, Kawaguchi, Saitama 332-0012, Japan

Supporting Information

ABSTRACT: Alkali-metal-ion extraction reactions using poly(tetrafluoroethylene) (PTFE; AEP reactions) were performed on two kinds of α-$NaFeO_2$-type layered compounds: $Na_{0.68}(Li_{0.68/3}Ti_{1-0.68/3})O_2$ and $K_{0.70}(Li_{0.70/3}Sn_{1-0.70/3})O_2$. At 400 °C in flowing argon, these layered compounds were reacted with PTFE. By these reactions, alkali-metal ions in the layered compounds were successfully extracted, and TiO_2 and SnO_2 with rutile-type structure were formed. The structural similarity between the alkali-metal-ion-extracted layered compounds and the binary metal oxide products in these unique alkali-metal-ion extraction reactions was interpreted in terms of their interatomic distance distribution by atomic pair distribution function analysis. The results of this study indicate that PTFE is an effective agent to extract alkali-metal ions from layered compounds, and AEP reaction is not limited to the previously reported γ-FeOOH-type layered titania $K_{0.8}(Li_{0.27}Ti_{1.73})O_4$, but is also applicable to other layered titania and other non-titanium-based layered metal oxides. Therefore, it was clarified that AEP reactions are widely applicable routes to prepare various compounds, including those that are difficult to synthesize by other reactions.

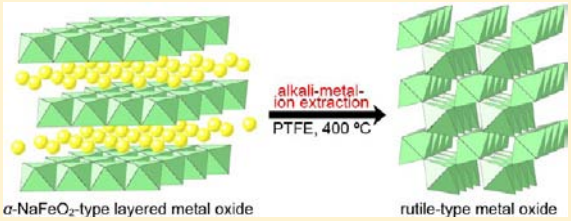

INTRODUCTION

Recently, we have succeeded in preparing single-phase brookite, which is a metastable phase, using a new reaction route.[1] Our reaction utilizes strong ionic interaction between alkali-metal ions in a γ-FeOOH-type layered compound $K_{0.8}(Li_{0.27}Ti_{1.73})O_4$ (KLTO) and F in poly(tetrafluoroethylene) (PTFE). When KLTO was reacted with PTFE at 400 °C in an inert atmosphere, K^+ and Li^+ in KLTO were extracted, forming alkali-metal fluorides, and the remaining unstable Ti−O-layered framework was transformed into brookite. On the basis of atomic pair distribution function (PDF) analysis, it was shown that the Ti−O layer in KLTO is structurally closest to brookite rather than other TiO_2 polymorphs such as anatase and rutile.[2] It is considered to be an important factor that the alkali-metal-ion-extracted KLTO was transformed into metastable brookite rather than other TiO_2 polymorphs. The brookite product at this stage includes PTFE and alkali-metal derivatives as impurity phases. However, those impurity phases can easily be removed by oxidative decomposition and dissolution in water for PTFE and alkali-metal derivatives, respectively. Thus, the single-phase brookite was successfully and easily synthesized through alkali-metal-ion extraction utilizing PTFE (AEP).

Conventionally, alkali-metal-ion extraction from a crystalline compound has been performed by methods such as soft-chemical[3−7] and electrochemical[8] reactions. Those conventional alkali-metal-ion extraction reactions can be used to synthesize various compounds including metastable ones. However, compounds prepared by the conventional alkali-metal-ion extraction reactions are mainly ion-exchanged, oxidized, reduced, or deintercalated phases. Thus, those product compounds tend to retain the fundamental structural frameworks of their precursors. On the contrary, in the case of the AEP reaction of KLTO, the alkali-metal-ion-extracted intermediate phase was quite unstable, and the reaction took place at the mid-temperature range of around 400 °C rather than lower or higher temperatures. Thus, the partial rearrangement of the structural framework took place to form a more stable, but metastable brookite phase, which is structurally related to its precursor. So far, the AEP reaction has been tested and reported only on KLTO. This AEP reaction may be applicable to various kinds of layered compounds other than KLTO to produce many interesting compounds including metastable ones, which are not possible or are difficult to prepare by other synthetic routes. Therefore, it is interesting and important to investigate the AEP reaction on various alkali-metal-ion-containing layered compounds and to further understand the structural relationship between the alkali-metal-ion-containing layered compounds and their AEP reaction products.

Received: April 4, 2012
Published: June 8, 2012

dx.doi.org/10.1021/ic3006986 | Inorg. Chem. 2012, 51, 7317−7323

In this paper, we report the results from the newly investigated AEP reactions on two kinds of α-$NaFeO_2$-type layered compounds: $Na_{0.68}(Li_{0.68/3}Ti_{1-0.68/3})O_2$ (NLTO)[9] and $K_{0.70}(Li_{0.70/3}Sn_{1-0.70/3})O_2$ (KLSO). The layer units in these compounds consist of edge-shared Li^+-substituted MO_6 (M = Ti^{4+}, Sn^{4+}) octahedra, and those layers are interspersed with Na^+ and K^+, respectively, for NLTO and KLSO. For NLTO, the focuses of the investigation are whether the AEP reaction is applicable to a layered titania with a structure other than that of KLTO and whether an alkali-metal ion other than K^+ and Li^+ can be extracted. On the other hand, for KLSO, the focus of the investigation is whether the AEP reaction is applicable to a non-titanium-based layered metal oxide.

EXPERIMENTAL PROCEDURE

Materials. The layered oxides NLTO and KLSO were prepared by solid-state reactions of metal oxides and alkali-metal carbonates in air. For NLTO, the starting materials in a stoichiometric mole ratio of 0.68/2:0.68/6:1−0.68/3 Na_2CO_3:Li_2CO_3:TiO_2 were mixed, placed in a capped platinum crucible, heated at 850 °C in air for 0.5 h, reground, and reheated at 900 °C in air for 24 h. Similarly, KLSO was prepared using the starting materials in a mole ratio of 0.70/2:0.70/6:1−0.70/3 K_2CO_3:Li_2CO_3:SnO_2. The mixture of these reactants was heated at 850 °C in air for 0.5 h, reground, and reheated at 1000 °C in air for 48 h.

Scheme 1. Alkaline-Metal-Ion Extraction and Oxide Product Phase Purification Process Sequences for (a) NLTO and (b) KLSO

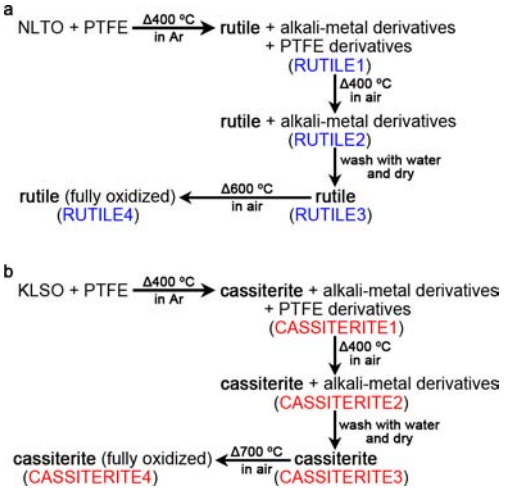

Then, AEP reactions were performed on these layered oxides NLTO and KLSO as in Scheme 1. First, alkali-metal-ion extraction was performed by reacting each layered oxide and PTFE powder in 1:2 mole ratio at 400 °C in 0.1 L/min flow of argon gas for 12 h. The products of these reactions for NLTO and KLSO are denoted as RUTILE1 and CASSITERITE1, respectively.

Second, RUTILE1 and CASSITERITE1 were reheated at 400 °C in 0.3 L/min flow of air in order to oxidatively decompose PTFE derivatives. The required heating duration depends on the amount of PTFE used (36 h for 0.6 g and 132 h for 2.9 g of PTFE). The products after PTFE derivative removal are denoted as RUTILE2 and CASSITERITE2, respectively.

Third, RUTILE2 and CASSITERITE2 were washed with copious amounts of water in order to dissolve and rinse out the coproduced alkali-metal derivatives. These washed phases are dried in air, and they are denoted as RUTILE3 and CASSITERITE3, respectively.

Finally, RUTILE3 and CASSITERITE3 were heated at 600 and 700 °C, respectively, for 12 h in 0.3 L/min flow of air in order to fully oxidize the products. These final products are denoted as RUTILE4 and CASSITERITE4, respectively.

Characterizations. Powder X-ray diffraction (XRD) profiles of NLTO, KLSO, and their reaction products were obtained using Cu Kα radiation on a Rigaku RINT2200V/PC diffractometer. The diffraction peaks were indexed, and the lattice parameters were refined using APPLEMAN software.[10] The elemental compositions of the reaction products were analyzed by flame atomic absorption spectrometry (FAAS), inductively coupled plasma-optical emission spectrometry (ICP-OES), and the lanthanum−alizarin complexone method for alkali metals (Li, Na, and K), other metals (Ti and Sn), and F, respectively (see the Supporting Information for details). Morphology analysis of the AEP reaction products was performed using a Keyence VE-8800 scanning electron microscope. Finally, atomic PDF profiles were calculated using the programs PDFfit2 and PDFgui.[11]

RESULTS AND DISCUSSION

The photographs and powder XRD profiles of NLTO, PTFE, and their reaction products are shown in Figures 1 and 2,

Figure 1. Photographs of NLTO, NLTO + PTFE, RUTILE1, RUTILE2, RUTILE3, and RUTILE4.

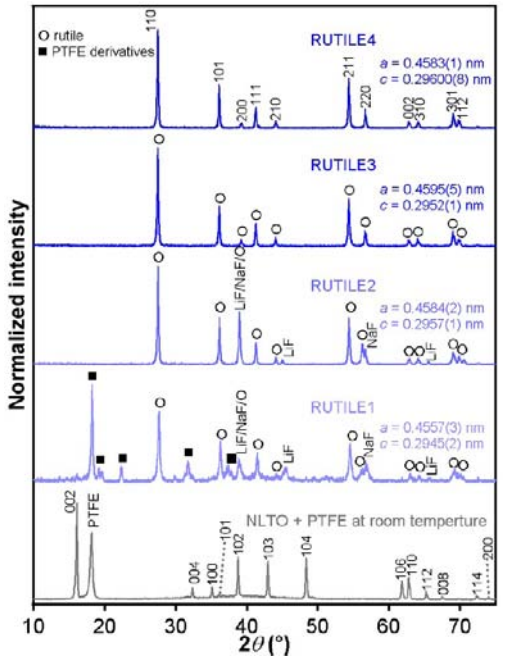

Figure 2. Powder XRD profiles of NLTO + PTFE, RUTILE1, RUTILE2, RUTILE3, and RUTILE4.

respectively. All of the diffraction peaks of NLTO were indexed based on its α-$NaFeO_2$-type structure; thus, it was single phase. The preheated mixture of NLTO and PTFE was white, and a diffraction peak of PTFE was clearly observed around 18° in 2θ. After heating of the mixture of NLTO and PTFE at 400 °C in argon, the color of the product (RUTILE1) turned to black. This black color is attributed to PTFE derivatives that tend to form when PTFE is heated in an inert atmosphere. RUTILE1 consists of a mixture of rutile (space group: $P4_2/mnm$), alkali-metal fluorides, and PTFE derivatives, and no trace of NLTO

dx.doi.org/10.1021/ic3006986 | Inorg. Chem. 2012, 51, 7317−7323

was observed in the diffraction profile. This result suggests that alkali-metal ions (Na^+ and Li^+) are successfully extracted from NLTO.

The PTFE derivatives in RUTILE1 were then decomposed by reheating in flowing air. After this process, the color of the product (RUTILE2) turned to light-bluish-gray. The disappearance of the black color indicates decomposition of PTFE derivatives from RUTILE1, and this is consistent with the XRD profile of RUTILE2, where peaks are only from rutile and alkali-metal fluorides.

In order to isolate the rutile phase in RUTILE2, RUTILE2 was washed in water and dried in air. The powder XRD profile of the product (RUTILE3) shows no peak from alkali-metal fluorides, which are water-soluble. Thus, single-phase rutile was successfully obtained through the mid-temperature AEP reaction of NLTO and the following easy purification processes. However, the color of RUTILE3 was still light-bluish-gray. For fully oxidized rutile, a white color was expected. The fact that the color of RUTILE2 and RUTILE3 was light-bluish-gray suggests that Ti^{4+} in RUTILE2 and RUTILE3 was partially reduced to the 3+ state, as occurs for reduced oxides due to the formation of oxygen deficiency and/or partial replacement of O^{2-} with F^-.[1] For example, in the case of oxygen-deficient rutile, a bluish-gray color was observed for $TiO_{1.984}$.[12]

Finally, RUTILE3 was oxidized by heating at 600 °C in air. The color of RUTILE4 was white, which indicated the formation of a fully oxidized rutile.

The lattice parameters of the intermediate and final rutile products estimated from the XRD data are shown in Figure 2. The lattice parameters of all of these rutile products agree with the previously reported lattice parameters of the rutile structure.[13] The lattice parameters of RUTILE1 are slightly smaller than those of RUTILE2, RUTILE3, and RUTILE4. Because the diffraction peaks of RUTILE1 are rather broad and not well-defined, such features might be causing the error in its estimated lattice parameters. Straumanis et al. reported that a slight reduction (color change) of rutile does not affect the lattice parameters significantly where the unit cell volume decrease because of the reduction of $TiO_{1.999}$ (yellowish white) to $TiO_{1.983}$ (bluish black) is as low as 0.0032%.[12] On the contrary, significant enlargement in the lattice parameters has been reported for heavily F^--doped rutile ($TiO_{2-x}F_x$, where $x \geq 0.3$).[14] Therefore, the oxygen deficiency and/or fluorination amounts in the rutile products in our study must be quite low.

The elemental compositions of the intermediate and final rutile products estimated by chemical analysis are summarized in Table 1. These compositions agree well with the XRD results. The remnant F in RUTILE1 was successfully removed by reheating in air. This removal of F is attributed mainly to the oxidative decomposition of the PTFE derivatives and partially to the oxidation of the rutile phase. The remaining F in RUTILE2 was mainly from alkali-metal fluoride phases NaF and LiF, which formed as a result of alkali-metal-ion extraction from NLTO using F-containing reagent PTFE. These extra elements in the forms of the alkali-metal fluorides in RUTILE2 were then removed by dissolving in water, and RUTILE3 contains only a trace level of alkali-metal elements and a much reduced amount of F. The remnant F in RUTILE3 is mainly attributed to partial fluorination of the O^{2-} site in the rutile product. That was why Ti in the rutile product was not totally in the 4+ state, but partially reduced to the 3+ state and RUTILE3 was not white, but light-bluish-gray. Such F^- as a dopant in the O^{2-} site of rutile can be removed by additional reheating at 600 °C in air. At this temperature in air, F^- in the O^{2-} site was replaced with O^{2-}, forming fully oxidized rutile (RUTILE4). The still remaining very low level F content in RUTILE4 might be from the residual alkali-metal fluorides because the mole ratio of F and the sum of Li and Na is 1:1 within the experimental uncertainty. Additional water treatment is likely effective in the further removal of the trace amount of such possible residual phases.

Table 1. Analytically Determined Molar Elemental Compositions of the Intermediate and Final Rutile Products Prepared from NLTO by the AEP Reaction

	Na	Li	Ti	F
NLTO[a]	0.8793	0.2931	1	
RUTILE1	0.89	0.29	1	4.6[b]
RUTILE2	0.90	0.30	1	1.2
RUTILE3	0.006	0.005[c]	1	0.017
RUTILE4	0.006	0.005[c]	1	0.009

[a]The elemental composition of NLTO is nominal based on its chemical formula, $Na_{0.68}(Li_{0.68/3}Ti_{1-0.68/3})O_2$. [b]The high content of F is attributed to the remaining PTFE and its derivatives. [c]These values are within the background range of the analysis.

In addition, scanning electron microscopy (SEM) images of the intermediate and final rutile products are shown in Figure 3. The crystallite size of NLTO is around 5 μm. After mixing with PTFE, about 10 μm particles with rough surfaces due to the surrounding nanometer-order PTFE powder were formed. Upon heating of the mixture in argon, the surface of the product (RUTILE1) particles became relatively smooth. This

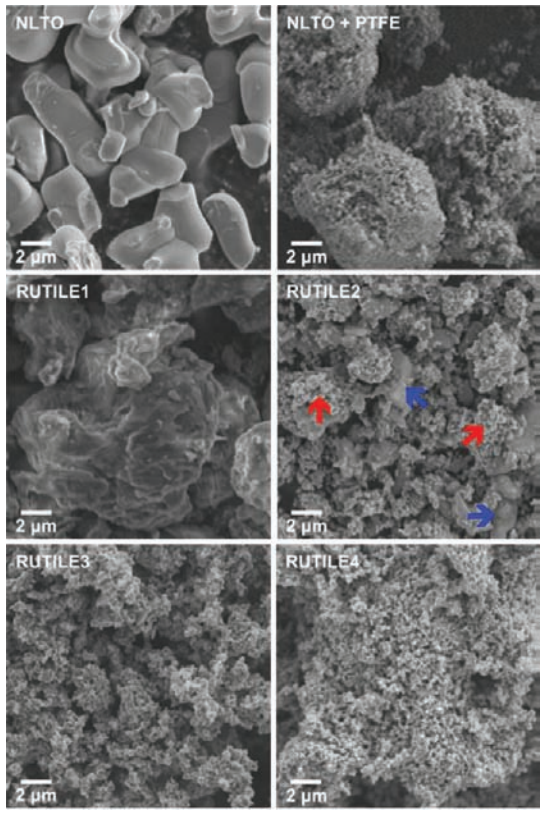

Figure 3. SEM images of NLTO, NLTO + PTFE, RUTIEL1, RUTILE2, RUTILE3, and RUTILE4.

dx.doi.org/10.1021/ic3006986 | Inorg. Chem. 2012, 51, 7317−7323

relatively smooth surface of RUTILE1 disappeared when it was reheated to form RUTILE2. Therefore, the relatively smooth surface of RUTILE1 is considered to be fused PTFE derivatives surrounding the rutile and alkali-metal fluoride products. RUTILE2 consists of aggregates of nanometer- and micrometer-order particles, which are indicated by red and blue arrows, respectively, in Figure 3. The latter disappeared when RUTILE2 was washed in water to form RUTILE3. Therefore, it must be the water-soluble alkali-metal fluorides. On the other hand, the nanometer-order particles observed in RUTILE2 must be rutile because its morphology is the same as that of RUTILE3, which is a single-phase rutile. Further reheating of RUTILE3 at 600 °C to form fully oxidized rutile (RUTILE4) did not alter the morphology of these two samples.

The AEP reaction of KLSO was similarly investigated. The photographs and powder XRD profiles of KLSO, PTFE, and their reaction products are shown in Figures 4 and 5,

Figure 4. Photographs of KLSO, KLSO + PTFE, CASSITERITE1, CASSITERITE2, CASSITERITE3, and CASSITERITE4.

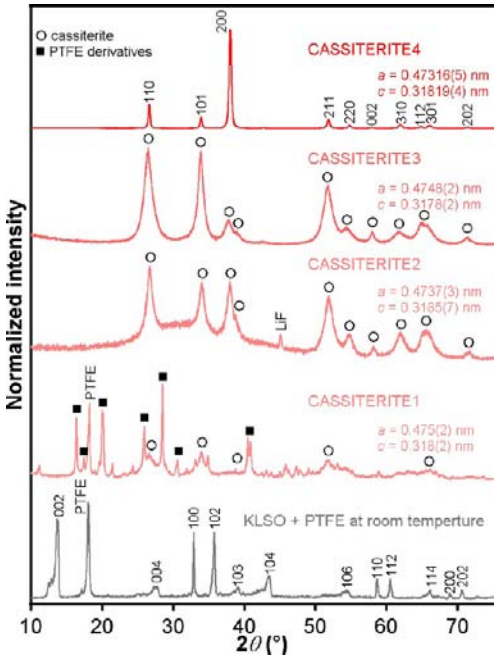

Figure 5. Powder XRD profiles of KLSO + PTFE, CASSITERITE1, CASSITERITE2, CASSITERITE3, and CASSITERITE4.

respectively. All of the diffraction peaks of KLSO were indexed based on its α-$NaFeO_2$-type structure; thus, it was single phase. The white mixture of KLSO and PTFE turned to black upon heating at 400 °C in flowing argon. XRD peaks of this product (CASSITERITE1) are mainly from cassiterite (SnO_2 with rutile-type structure)[15] and PTFE derivatives, and no peak from KLSO was observed. This result suggests that alkali-metal ions (K^+ and Li^+) in KLSO were successfully extracted by this reaction.

CASSITERITE1 was then reheated in a flow of air in order to oxidatively decompose PTFE derivatives. The product (CASSITERITE2) was brownish-gray, and its diffraction peaks were only from cassiterite and alkali-metal fluorides, indicating the successful removal of PTFE derivatives.

CASSITERITE2 was then washed in water in order to dissolve alkali-metal fluorides and dried in air. The XRD profile of the product (CASSITERITE3) consists of peaks only from cassiterite, indicating the successful removal of alkali-metal fluorides. The cassiterite phase at this stage was still brownish-gray in color, not the white expected for fully oxidized cassiterite. The brownish-gray color of CASSITERITE3 is attributed to partial fluorination and/or deficiency of the O^{2-} site in the cassiterite crystal structure like the case for the bluish-gray color of rutile prepared from NLTO in this study.

Upon heating of CASSITERITE3 at 700 °C in flow of air, the color of the product (CASSITERITE4) turned to white, indicating successful full oxidation. In addition, the diffraction peaks from CASSITERITE4 were much narrower than those from CASSITERITE3, indicating increased crystallinity upon heat treatment at 700 °C. More noticeably, CASSITERITE4 shows a significant preferred orientation along the *h*00 direction. The diffraction profile of CASSITERITE3 is very close to that calculated from the crystal structure of the cassiterite phase with random crystallite orientations, and the 110 reflection has the highest intensity. On the other hand, the 200 reflection intensity from CASSITERITE4 is much higher than those from other reflections. As discussed later with the result of the SEM observation, this unusual relative diffraction intensity of CASSITERITE4 is attributed to the crystallite morphology change in the final oxidation of CASSITERITE3 to CASSITERITE4.

The lattice parameters *a* and *c* of cassiterite in CASSITERITE1, CASSITERITE2, CASSITERITE3, and CASSITERITE4 agreed well with previously reported values,[15] and their differences were less than 0.4% (Figure 5). These small differences in the lattice parameters indicate that fluorination and/or deficiency, if they exist, in O^{2-} sites of the cassiterite structures in CASSITERITE1, CASSITERITE2, and CASSITERITE3 are trace amounts.

The SEM images of KLSO, PTFE, and their reaction products are shown in Figure 6. As-prepared KLSO crystallites were 10−50 μm in size. After KLSO was mixed with PTFE, the KLSO crystallites were fully covered with nanometer-order particles of PTFE. After heating of the mixture of KLSO and PTFE at 400 °C in a flow of argon, the majority of CASSITERITE1 particles had sizes of around 10−40 μm, and their surfaces were quite rough. Considering the XRD results, the main body of these CASSITERITE1 particles must be cassiterite, and PTFE derivatives and alkali-metal fluorides form the rough surface. Upon reheating of CASSITERITE1 at 400 °C in air, the surface of CASSITERITE2 became a little smoother than that of CASSITERITE1. This change is attributed to the removal of the surface PTFE derivatives by oxidative decomposition. CASSITERITE2 was then washed in water in order to remove alkali-metal fluorides on the CASSITERITE2 particle surfaces. The surface of the resulting CASSITERITE3 (single-phase cassiterite) became much smoother than that of CASSITERITE2, indicating the successful removal of the alkali-metal fluorides from KLSO. In addition, two-dimensional crevices were observed in the crystallites of CASSITERITE3. CASSITERITE3 is a single-phase cassiterite, which has a three-dimensional crystal structure. However, the observed morphology of CASSITERITE3 looks as if CASSITERITE3 is a layered compound because of its crevices. This might be an indication that the

dx.doi.org/10.1021/ic3006986 | Inorg. Chem. 2012, 51, 7317−7323

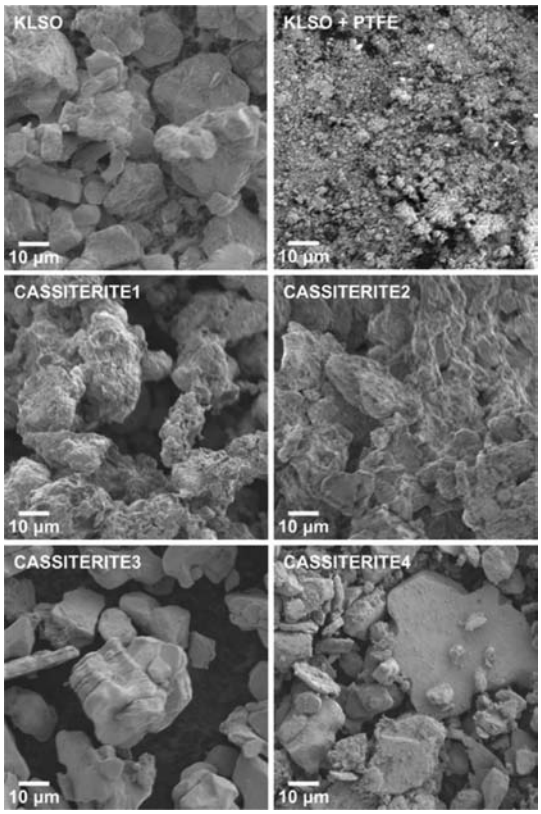

Figure 6. SEM images of KLSO, KLSO + PTFE, CASSITERITE1, CASSITERITE2, CASSITERITE3, and CASSITERITE4.

AEP reaction took place without significantly altering the stacked-layer nature of the alkali-metal-ion-containing starting material KLSO. Finally, CASSITERITE3 was reheated at 700 °C in air in order to fully oxidize it into CASSITERITE4. After the final oxidation, the crevices of crystallites disappeared. In addition, some of the crystallites were larger than those found in CASSITERITE3. These changes in the morphology and preferred orientation along the *a* axis of CASSITERITE4 in the powder XRD profile indicate that the stacked-layer morphology kept up to CASSITERITE3 was no longer retained during the final oxidation process at higher temperature. At 700 °C, the oxidized cassiterite crystallite in this study preferably grew in the direction perpendicular to the *a* axis, in contrast to the general growth direction of rutile along the *c* axis.[16] This pronounced morphology transformation at high temperature might be originating from the unique aspect of the AEP reaction products for which significant F^- doping and/or oxygen deficiency was introduced. In fact, this unique transformation was not observed in the case of the AEP reaction products of NLTO, whose remnant F content was much lower than that of KLSO.

The elemental compositions of the intermediate and final cassiterite products are summarized in Table 2. A large amount of F was observed in CASSITERITE1 originating from PTFE derivatives and alkali-metal fluorides. After decomposition of the PTFE derivatives by heating in a flow of air, the product CASSITERITE2 contained much less F. The remaining F content must be primarily due to the alkali-metal fluoride components in CASSITERITE2. Such alkali-metal fluorides were successfully washed out by rinsing CASSITERITE2 in water to form a single-phase cassiterite (CASSITERITE3). CASSITERITE3 was not white, but brownish-gray. We believe

Table 2. Analytically Determined Molar Elemental Compositions of the Intermediate and Final Cassiterite Products Prepared from KLSO by the AEP Reaction

	K	Li	Sn	F
KLSO[a]	0.9130	0.3043	1	
CASSITERITE1	0.88	0.30	1	4.9[b]
CASSITERITE2	0.84	0.32	1	1.3
CASSITERITE3	0.014	0.04	1	0.1
CASSITERITE4	0.008	0.05	1	0.02

[a]The elemental composition of KLSO is nominal based on its chemical formula, $K_{0.70}(Li_{0.70/3}Sn_{1-0.70/3})O_2$. [b]The high content of F is attributed to the remaining PTFE and its derivatives.

that O^{2-} sites in CASSITERITE3 are partially fluorinated and/or oxygen deficiency exists; thus, Sn^{4+} in CASSITERITE3 is likely slightly reduced. The small, but finite amount of F still remaining in CASSITERITE3 is consistent with the expectation. Such remaining F in CASSITERIE3 can be further removed by oxidative heating at 700 °C in flowing air. The final product CASSITERITE4 contained only a trace level of F. The still remaining very low level F content in CASSITERITE4 might be from the residual alkali-metal compounds. Additional water treatment is likely to be effective in the further removal of the trace amount of such possible residual phases.

These experimental results from the mid-temperature AEP reactions of NLTO and KLSO clearly proved that AEP process is not only applicable to the previously reported γ-FeOOH-type titania (KLTO),[1] but also applicable to other alkali-metal ion containing layered compounds with different structure types and non-Ti-based metal oxides. In addition, all the alkali-metal ion extracted oxides prepared by the AEP reactions of KLTO, NLTO and KLSO can easily be purified into single-phase products by subsequent thermal decomposition of PTFE derivatives, water-washout of alkali-metal derivatives, and removal of oxygen deficiency and/or F^--dopant by heat treatment at higher temperature than the mid-temperature around 400 °C of the AEP reactions. Thus, it is likely that the AEP reaction is a widely applicable route to extract alkali-metal ions from layered metal oxides and to uniquely prepare single-phase metal oxide compounds, including metastable oxides such as brookite.

In order to choose an appropriate alkali-metal-ion-containing layered compound as a precursor to produce a particular oxide product in such an AEP reaction, it is important to understand the structural relationship between alkali-metal-ion-containing layered oxide precursors and their AEP reaction products. As was previously reported, in the case of the transformation of KLTO into brookite by the AEP reaction, close structural similarity between the alkali-metal-ion-extracted Ti−O layer of KLTO and the brookite product was clarified by atomic PDF analysis of their crystal structures in terms of statistical distributions of interatomic distances.[1,2] Therefore, we performed similar atomic PDF calculations on the structures of alkali-metal-ion-extracted NLTO and TiO_2 polymorphs. Figure 7 shows the calculated atomic PDF profiles of the Ti−O layer of the alkali-metal-ion-extracted NLTO and three major polymorphs of TiO_2: brookite,[17] anatase,[18] and rutile.[15] The structures of the Ti−O layer of NLTO and all of these polymorphs of TiO_2 consist of edge- and/or corner-shared TiO_6 octahedral linkages (Figure 8). Therefore, the calculated atomic PDF profiles of these phases have large peaks around 0.2 nm representing the distribution of the closest Ti−O

dx.doi.org/10.1021/ic3006986 | Inorg. Chem. 2012, 51, 7317−7323

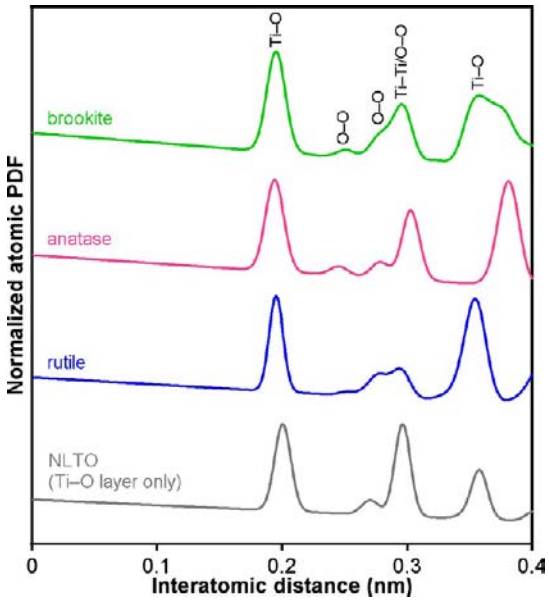

Figure 7. Calculated atomic PDF profiles of NLTO (Ti–O layer only), rutile, anatase, and brookite. The characteristic interatomic pairs are indicated.

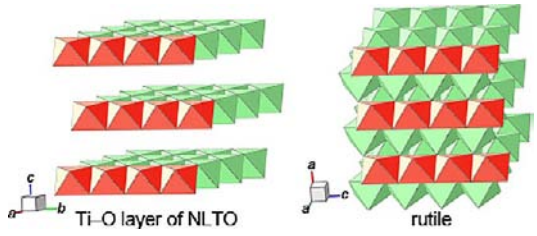

Figure 8. Crystal structures of alkali-metal-ion-extracted NLTO and rutile.

distance in their structures. The atomic PDF profile of the Ti–O layer of the alkali-metal-ion-extracted NLTO is closest to that of rutile among these atomic PDF profiles of the TiO_2 polymorphs. There are two characteristic similarities between those two closely related Ti–O structures. First, the structure of the Ti–O layer of NLTO does not have distribution of the O–O interatomic distance around 0.25 nm, and the rutile structure has the lowest distribution of the O–O distance in this range among the three polymorphs of TiO_2. Second, the structure of the Ti–O layer of NLTO has a relatively high distribution of the Ti–O distance around 0.36 nm, and the rutile has a similar Ti–O distance distribution. On the other hand, the structures of anatase and brookite have different distributions of the Ti–O distance. The Ti–O distance in the anatase structure is larger around 0.38 nm, and that in the brookite structure is widely distributed from 0.35 to 0.38 nm. Therefore, the structure of the Ti–O layer of the alkali-metal-ion-extracted NLTO is closest to that of rutile in terms of the interatomic distance distributions.

Furthermore, this structural similarity between the alkali-metal-ion-extracted NLTO and rutile can visually be confirmed. As shown in Figure 8 in red, both the alkali-metal-ion-extracted NLTO and rutile have edge-shared linkages of TiO_6 octahedra. This feature does not exist in the structures of the other TiO_2 polymorphs. This aspect again suggests that the alkali-metal-ion-extracted NLTO transforms into the structurally closest TiO_2 phase at 400 °C during the AEP process, and the same structural relationship applies to KLSO and its AEP reaction product, cassiterite, because KLSO is isostructural with NLTO and cassiterite is isostructural with rutile. In fact, this transformation from alkali-metal-ion-extracted layered intermediates to rutile-type binary oxides might be quasi-topotactic, as indicated by the crevices in CASSITERITE3 crystallites.

All of the investigated layered compounds (NLTO, KLSO, and KLTO) in this and previous studies transform into the phases that are structurally closest to the alkali-metal-ion-extracted layered compound reactants. This result implies that these reactions are nonequilibrium processes utilizing the mid-temperature modification of the structural framework of the alkali-metal-ion-extracted layered compounds as foundations. In addition, the new results suggest that AEP reactions are not only applicable to the previously reported γ-FeOOH-type titania (KLTO), but also applicable to other alkali-metal-ion-containing layered compounds with different structure types and non-Ti-based metal oxides. Furthermore, as long as a product and an alkali-metal-ion-extracted reaction intermediate are structurally close, a metastable product can be prepared utilizing the AEP reaction.[1]

In general, PTFE is quite inert; thus, it is often used as a reaction container material. Rare examples of the PTFE reaction with oxides are previously reported for the partial replacement of O^{2-} or filling of oxygen deficiencies with F^-.[19−23] However, the results from our studies indicate that PTFE can also be used to extract alkali-metal ions from layered compounds with appropriate conditions such as the reaction temperature and atmosphere. The strong ionic interaction between highly electropositive alkali metals in the layered compound precursors and highly electronegative F in PTFE must be the driving force of these AEP reactions. These clarified features of the AEP reactions provide a guideline to preparing various compounds using the AEP reaction. The first step in such an approach is to look for an alkali-metal-ion-containing compound as a precursor that is structurally close to a desired product phase; thus, it is a retrosynthetic approach. The AEP reaction can be performed on such a precursor compound, and the product can easily be purified by further heating in air and rinsing in water. Therefore, this is an innovative approach to preparing various single-phase materials. Investigations of various retrosynthesis utilizing AEP reactions are underway in order to prepare new compounds, which cannot be prepared by other synthetic routes, and to further prove the usefulness of the AEP reaction.

SUMMARY AND CONCLUSION

AEP reactions were newly performed on two kinds of layered compounds: NLTO and KLSO. As reported previously for KLTO, alkali-metal ions were successfully extracted from NLTO and KLSO by the AEP reactions. The alkali-metal-ion-extracted NLTO and KLSO transformed into rutile and cassiterite, respectively. Both rutile and cassiterite have the same crystal structure, which is closest to that of the alkali-metal-ion-extracted NLTO and KLSO among their polymorphs. It is this structural similarity that is attributed to the formation of rutile and cassiterite from NLTO and KLSO, respectively, rather than other polymorphs of the binary metal oxides. By considering such structural similarity as the key aspect, the AEP reaction can be used in a retrosynthetic way in order to prepare various new compounds, including metastable ones, from alkali-metal-ion-containing precursor compounds.

dx.doi.org/10.1021/ic3006986 | Inorg. Chem. 2012, 51, 7317−7323

■ ASSOCIATED CONTENT

Supporting Information

Elemental composition analysis procedure for the AEP reaction products of NLTO and KLSO. This material is available free of charge via the Internet at http://pubs.acs.org.

■ AUTHOR INFORMATION

Corresponding Author

*E-mail: OZAWA.Tadashi@nims.go.jp.

Notes

The authors declare no competing financial interest.

■ ACKNOWLEDGMENTS

We thank Dr. K. Takada for use of his research facility. This work was, in part, supported by World Premier International Research Center Initiative (WPI), MEXT, Japan, and CREST of JST. The schematic crystal structure in Figure 8 was drawn using "Balls & Sticks", free software for crystal structure visualization.[24]

■ REFERENCES

(1) Ozawa, T. C.; Sasaki, T. *Inorg. Chem.* **2010**, *49*, 3044.
(2) Gateshki, M.; Yin, S.; Ren, Y.; Petkov, V. *Chem. Mater.* **2007**, *19*, 2512.
(3) Sasaki, T.; Kooli, F.; Iida, M.; Michiue, Y.; Takenouchi, S.; Yajima, Y.; Izumi, F.; Chakoumakos, B. C.; Watanabe, M. *Chem. Mater.* **1998**, *10*, 4123.
(4) Stein, A.; Keller, S. W.; Mallouk, T. E. *Science* **1993**, *259*, 1558.
(5) Gopalakrishnan, J. *Chem. Mater.* **1995**, *7*, 1265.
(6) Cheetham, A. K. *Science* **1994**, *264*, 794.
(7) Gopalakrishnan, J.; Bhuvanesh, N. S.; Rangan, K. K. *Curr. Opin. Solid State Mater. Sci.* **1996**, *1*, 285.
(8) Chiba, K.; Kijima, N.; Takahashi, Y.; Idemoto, Y.; Akimoto, J. *Solid State Ionics* **2008**, *178*, 1725.
(9) Shilov, G. V.; Nalbandyan, V. B.; Volochaev, V. A.; Atovmyan, L. O. *Int. J. Inorg. Mater.* **2000**, *2*, 443.
(10) Appleman, D. E.; Evans, H. T., Jr. Indexing and least-squares refinement of powder diffraction data (Job 9214). *U.S. Geological Survey Computer Contribution No. 20*; PB National Technical Information: Springfield, VA, 1973; p 60.
(11) Farrow, C. L.; Juhas, P.; Liu, J. W.; Bryndin, D.; Božin, E. S.; Bloch, J.; Proffen, T.; Billinge, S. J. L. *J. Phys.: Condens. Matter* **2007**, *19*, 335219.
(12) Straumanis, M. E.; Ejima, T.; Janes, W. J. *Acta Crystallogr.* **1961**, *14*, 493.
(13) Restori, R.; Schwarzenbach, D.; Schneider, J. R. *Acta Crystallogr., Sect. B* **1987**, *43*, 251.
(14) Endo, T.; Morita, N.; Sato, T.; Shimada, M. *J. Mater. Res.* **1988**, *3*, 392.
(15) Baur, W. H.; Khan, A. A. *Acta Crystallogr., Sect. B* **1971**, *B27*, 2133.
(16) Harwood, M. G. *Brit. J. Appl. Phys.* **1965**, *16*, 1493.
(17) Pauling, L.; Sturdivant, J. H. *Z. Kristallogr.* **1928**, *68*, 239.
(18) Cromer, D. T.; Herrington, K. *J. Am. Chem. Soc.* **1955**, *77*, 4708.
(19) Slater, P. R. *J. Fluorine Chem.* **2002**, *117*, 43.
(20) Kobayashi, Y.; Tian, M.; Eguchi, M.; Mallouk, T. E. *J. Am. Chem. Soc.* **2009**, *131*, 9849.
(21) Heap, R.; Slater, P. R.; Berry, F. J.; Helgason, O.; Wright, A. J. *Solid State Commun.* **2007**, *141*, 467.
(22) Berry, F. J.; Ren, X.; Heap, R.; Slater, P.; Thomas, M. F. *Solid State Commun.* **2005**, *134*, 621.
(23) Baikie, T.; Young, N. A.; Francesconi, M. G. *Prog. Solid State Chem.* **2007**, *35*, 265.
(24) Ozawa, T. C.; Kang, S. J. *J. Appl. Crystallogr.* **2004**, *37*, 679.